Terahertz superconductor metamaterial

Jianqiang Gu,[1,2] Ranjan Singh,[1,3] Zhen Tian,[1,2] Wei Cao,[1] Qirong Xing,[2] Mingxia He,[2] Jingwen W. Zhang,[4] Jiaguang Han,[2,5] Hou-Tong Chen,[3] and Weili Zhang[1,a)]
[1]*School of Electrical and Computer Engineering, Oklahoma State University, Stillwater, Oklahoma 74078, USA*
[2]*Center for Terahertz Waves and College of Precision Instrument and Optoelectronics Engineering, The Key Laboratory of Optoelectronics Information and Technical Science (Ministry of Education), Tianjin University, Tianjin 300072, People's Republic of China*
[3]*Center for Integrated Nanotechnologies, Materials Physics and Applications Division, Los Alamos National Laboratory, Los Alamos, New Mexico 87545, USA*
[4]*Department of Physics, Harbin Institute of Technology, Harbin 150001, People's Republic of China*
[5]*Department of Physics, National University of Singapore, 2 Science Drive 3, Singapore 117542*

(Received 9 May 2010; accepted 23 July 2010; published online 16 August 2010)

We characterize the behavior of split ring resonators made up of high transition temperature yttrium barium copper oxide superconductor using terahertz time-domain spectroscopy measurements and numerical simulations. The superconductor metamaterial is found to show a remarkable change in the transmission spectra at the fundamental inductive-capacitive resonance as the temperature dips below the critical transition temperature. This resonance switching effect is normally absent in traditional metamaterials made up of regular metals. The temperature-dependent resonance behavior of the superconducting metamaterial would lead to development of low loss terahertz switches at cryogenic temperatures. © *2010 American Institute of Physics*. [doi:10.1063/1.3479909]

The emergence of metamaterials (MMs) has opened a gateway to unprecedented electromagnetic properties and functionality unattainable from naturally occurring materials, thus enabling a family of MM based devices such as superlens,[1,2] sensors,[3–5] cloak,[6] chiral devices,[7,8] electromagnetically induced transparency components for slow light[9,10] and modulators.[11,12] However, in spite of these and other advances, progress toward practical implementation of MM devices, particularly at higher frequencies, has been hampered by high absorption losses. A large majority of existing MM designs rely on the use of metallic structures sitting on a dielectric substrate. As the frequency of operation is pushed higher toward the terahertz (THz), infrared, and visible, the Ohmic losses quickly render the current MM approaches impractical. Thus, a top priority is to reduce the absorption losses to levels suitable for device applications. This would require MM designs that do not depend solely on metallic structures. One approach would be to utilize zero resistance superconductors as the MM constituent media which allow dissipation less flow of electrical current.

High transition temperature (Tc) superconductors (HTSs) (Ref. 13), discovered over twenty years back, promised to conduct electric current without resistance at liquid nitrogen temperature, but they still present tremendous challenge to our understanding. Recently, the cuprate (copper-oxide) HTS materials have shown great potential for applications in the design of low loss MMs. Ricci *et al.*[14] fabricated yttrium barium copper oxide (YBCO) MM and studied its tunability under magnetic field control at microwave frequencies. Fedotov *et al.*[15] showed the Fano resonances in microwave YBCO MM and observed the interaction between electric and magnetic dipoles. Thus, most of the previous works on superconductor MMs were focused in the microwave regime.

In this letter, we investigate the response of YBCO MM to THz radiation using a liquid helium cryostat installed in a THz time-domain spectroscopy (TDS) system[16] and numerical simulations. Interestingly, the real part of the conductivity of YBCO in the THz regime lies between that of a dielectric and good metal and is on the order of 10^5–10^6 S/m while its temperature is varied from room temperature to Tc. Using liquid helium cryogenics, the transition from normal state to superconducting state can be achieved in YBCO HTS which makes it really attractive for the development of temperature controlled THz devices. We measured the response of YBCO single split-ring resonators (SRRs) fabricated on sapphire substrate at different temperatures under normal incidence with the THz electric field oriented along the gap arm of the SRR. This incident field excites circulating currents in the SRRs at lower frequency giving rise to the inductive-capacitive (LC) resonance and linear currents at higher frequency resulting in the quadrupole resonance.[17–24] This quadrupole resonance is different from the dipole resonance which can be excited by rotating the SRR by 90°. In the quadrupolar mode resonance case the current in the two wire piece forming the gap side of SRR flows in opposite directions when compared at the lower frequency LC resonance and the higher frequency resonance thus forming a quadrupole current distribution.[25,26] The modulation of LC and quadrupole resonances is clearly observed as the temperature dips below the transition value of the superconductor. The two-fluid model is applied to analyze the changes in transmission resonances and based on this assumption the full-wave CST simulations could reproduce the experimental observations. The two-fluid model treats the conductivity of superconductor as composed of two following parts: one that is due to normal carriers whose motion is governed by the Drude theory and the other that is due to superconducting carriers whose motion is determined by the London equation.[27,28]

a)Electronic mail: weili.zhang@okstate.edu.

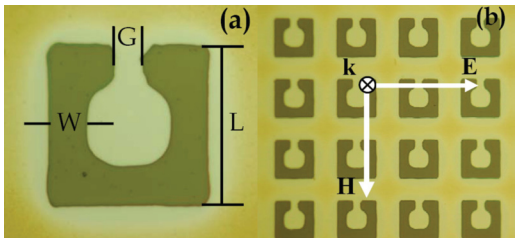

FIG. 1. (Color online) Microcopic image of (a) YBCO MM unit cell with structural parameters, W=8 μm, G=5 μm, and L=32 μm and (b) MM array with a periodicity of P=52 μm. The incident E field is polarized parallel to the gap of the single SRRs.

The MM sample was lithographically fabricated from a commercially available 280-nm-thick YBCO film which typically has Tc=86 K and to a critical current of 2.3 MA/cm^2 maximum current grown on a 500 μm thick sapphire substrate (THEVA, Germany). A 3-μm-thick photoresist layer was first patterned on the raw YBCO film as an etching protector. The sample was then wet etched in 0.1% nitric acid for 1 min followed by rinsing process in deionized water. The size of the sample array is 5 mm $\times$5 mm with SRR periodicity P=52 μm, and the structural dimensions of unit cells are length L=32 μm, width W =8 μm, and gap G=5 μm, as shown in the microscopic images in Figs. 1(a) and 1(b). The sample was measured in a standard liquid helium cryostat installed in the THz-TDS system.[21] The THz beam was focused to a 2.0 mm diameter waist to ensure a measurement without frequency filtering and the beam approximately covered 1200 SRRs. The sample was set with the SRR gap along the incident E field in order to excite the fundamental LC mode resonance and the quadrupole resonance. A bare sapphire substrate was used as the reference for all sets of measurements. The transmitted sub-picosecond THz pulses through both the sample and reference were measured at various temperatures between 297–27.4 K in time domain. The frequency-dependent transmission is defined as $|E_s(\omega)/E_r(\omega)|$, where $E_s(\omega)$ and $E_r(\omega)$ are the Fourier transform of the averaged time-domain sample and reference signals, respectively. The high temperature YBCO superconductor film has an energy gap of 30 meV and the energy range of the THz photons generated in our set up is typically between 1–10 meV which is well below the maximum energy gap values, making our measurements ideal without breaking apart the Cooper pairs.

By filling the vacuum chamber with liquid helium, the sample and the reference were characterized at 297 K, 200 K, 150 K, 100 K, 85 K, 51.4 K, and 27.4 K, respectively. The measured time-domain pulses, as shown in Fig. 2(a) reveal the dramatic change in the pulse shape upon cooling the sample from room temperature to well below the superconducting temperature. The reshaping of the pulse trail implies the amplitude and phase modulation at resonance frequencies, which is a direct consequence of superconductor's kinetic inductance. Such inductance is entirely due to the superconducting carrier's kinetics since a pure superconductor acts as an ideal inductor and the impedance of which is zero for dc current and imaginary for ac current, however, no power is dissipated through imaginary impedance. It physically means that as the superconductor reaches Tc, there is formation of Cooper pairs which are the superconducting carriers and the YBCO film becomes superconducting. Figure 2(b) shows the temperature-dependent amplitude transmission spectra. At room temperature, the LC and quadrupole resonances appear to be extremely weak due to low conductivity of YBCO. As the temperature is decreased toward Tc, the resonance evolves slowly and becomes more pronounced due to increased current flow in the superconductor film. The resonance shows a switching effect at temperatures lower than Tc. At 27.4 K, the LC and quadrupole resonances reach 0.49 and 0.21 with Q factors of 5.3 and 14.5, respectively. The phase modulation controlled by temperature change can be seen in Fig. 2(c). Our measurements reveal a sharp phase change centered at the LC and quadrupole resonances. The phase change at the first resonance is 0.66 rad and the change at second resonance is 1.04 rad. Consistent with the Kramers–Kronig relations, the measured transmission magnitude has the shape of the derivative of this peak. It highlights the consistency of both the measured phase and the amplitude transmission. Figure 2(d) shows the change in amplitude transmission at the LC and quadrupole resonances with decreasing temperatures. A noteworthy feature is that the sharpest change occurs when the temperature of the YBCO MM is decreased from 85 to 51.4 K, thus the transmission at the LC resonance sharply dropping from 0.75 to 0.53. The temperature-dependent amplitude modulation achieved at both the LC and quadrupole resonances is nearly absent in the regular MMs composed of thin metal films as the conductivity of metals cannot be modified like that of a system.[21]

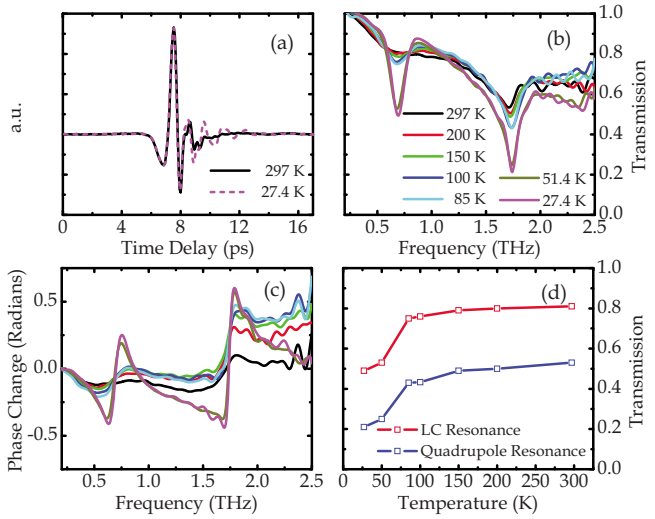

FIG. 2. (Color online) Measured (a) subpicosecond transmitted pulses through the MM at 297 and 27.4 K, (b) amplitude transmission spectra, (c) phase change spectra, and (d) percentage amplitude transmission at different low temperatures.

The amplitude and phase modulation of the THz transmission primarily originates from the temperature-dependent conductivity in the superconductor MMs. As the conductivity increases with decreasing temperature, the magnitude of circular currents at the LC resonance and the linear currents at the quadrupole resonance increases, resulting in strengthening of both resonances. According to the two-fluid model, the real part of the conductivity (σ_r) of YBCO is contributed by the normal state carriers whose motion follows Drude model while the imaginary part (σ_i) is determined by the superconducting carriers, which follow the London Equation,[27] where the conductivity of the superconducting carriers can be described as $\sigma_i = i(n_S e^2)/(m^*\omega)$, n_S is the Cooper pair carrier density, e is the charge of carriers, m^* is the

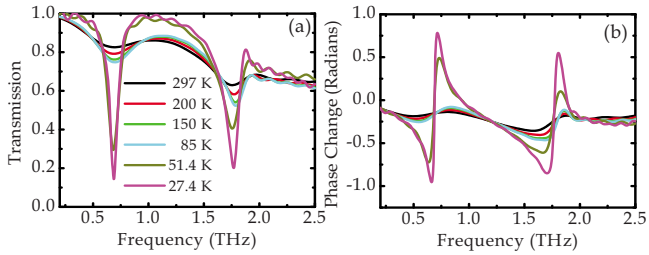

FIG. 3. (Color online) Simulated (a) amplitude and (b) phase transmission spectra of the YBCO MM above and below Tc.

effective carrier mass, and ω is the frequency of operation. It should be noted that the conductivity due to Cooper pairs is purely imaginary and thus the resistivity of the YBCO below Tc is also nearly imaginary, resulting in an inductor type behavior under the applied THz field. In the THz regime, at temperatures higher than Tc the real part of conductivity is dominant since the absolute value of the imaginary conductivity is three orders of magnitude less than the real part. However, starting from several kelvins under Tc the imaginary conductivity value rises drastically with falling temperatures and the total conductivity is then dominated by σ_i. We measured the direct THz transmission through an unpatterned 280-nm-thick YBCO film and extracted the real part of conductivity at 297 K, 200 K, 150 K, and at 85 K, respectively. No obvious frequency dependence is observed, but as the temperature goes down, σ_r increases from 3.6×10^5 S/m at 297 K to 7.1×10^5 S/m at 85 K.

Previous work on THz conductivity of YBCO film has shown that σ_i increases dramatically and exceeds the real part at several kelvins below Tc.[28] The sharp rise in the imaginary conductivity is signature of the onset of superconductivity and it can serve as an independent method to determine the superconducting Tc. As temperature goes down below Tc, the current in SRR grows stronger due to the superconducting carriers and results in sharp switching at LC and quadrupole resonances. In order to confirm our measurements at temperatures above and well below Tc, finite-element simulations using CST MICROWAVE STUDIO were carried out.[28] The simulated amplitude transmission shown in Fig. 3(a) also demonstrates the switching effect at both the resonances as temperature reaches well below Tc at 51.4 and 27.4 K.

The difference in modulation depth at resonances between simulation and experiments could be due to wet etching process in the sample fabrication, which is very sensitive to etching time and one could easily change the thickness of the superconductor film or the feature size of the SRRs. In addition, the most fundamental characteristic that makes HTS superconductors attractive for several applications is its ability to carry current without losses. The use of these superconductor films can be one of the paths to minimize the losses in MMs, however the quality of YBCO film used highly depends on dopant species, growth conditions, the composition, process optimization, and substrate preparation. The critical current density in YBCO is greatly limited by material imperfections such as cracks, voids, or secondary phases that partially block the current flow. Another factor that limits the current flow is the increasing misorientation angle between the adjacent grains. These defects lead to the losses in the superconductor MM and prevent the SRRs from supporting extremely high Q resonances. However, the measurements and simulations at 51.4 and 27.4 K clearly reveal a switching effect in the SRR behavior below Tc due to creation of high density Cooper pair superfluid.

The authors thank J. Wu for help in YBCO films and K. Dani and A. Azad for stimulating discussions. This work was supported by the U.S. National Science Foundation (Grant No. ECCS-0725764), The National Science Foundation of China (Grant No. 60977064), The National Key Basic Research Special Foundation of China (Grant Nos. 2007CB310403 and 2007CB310408), The Tianjin Sci-Tech Support Programs (Grant Nos. 08ZCKFZC28000, 09ZCKFGX01500, and 10JCYBJC01400), The MOE Academic Research Fund of Singapore, and the Lee Kuan Yew Fund. This work was performed, in part, at the Center for Integrated Nanotechnologies, a US Department of Energy, Office of Basic Energy Sciences Nanoscale Science Research Center operated jointly by Los Alamos and Sandia National Laboratories.

[1] J. B. Pendry, Phys. Rev. Lett. **85**, 3966 (2000).
[2] N. Fang, H. Lee, C. Sun, and X. Zhang, Science **308**, 534 (2005).
[3] C. Debus and P. H. Bolivar, Appl. Phys. Lett. **91**, 184102 (2007).
[4] J. F. O'Hara, R. Singh, I. Brener, E. Smirnova, J. Han, A. J. Taylor, and W. Zhang, Opt. Express **16**, 1786 (2008).
[5] I. A. I. Al-Naib, C. Jansen, and M. Koch, Appl. Phys. Lett. **93**, 083507 (2008).
[6] R. Liu, C. Ji, J. J. Mock, J. Y. Chin, T. J. Cui, and D. R. Smith, Science **323**, 366 (2009).
[7] S. Zhang, Y. S. Park, J. Li, X. Lu, W. Zhang, and X. Zhang, Phys. Rev. Lett. **102**, 023901 (2009).
[8] R. Singh, E. Plum, C. Menzel, C. Rockstuhl, A. K. Azad, R. A. Cheville, F. Lederer, W. Zhang, and N. I. Zheludev, Phys. Rev. B **80**, 153104 (2009).
[9] R. Singh, C. Rockstuhl, F. Lederer, and W. Zhang, Phys. Rev. B **79**, 085111 (2009).
[10] S. Y. Chiam, R. Singh, C. Rockstuhl, F. Lederer, W. Zhang, and A. A. Bettiol, Phys. Rev. B **80**, 153103 (2009).
[11] H. T. Chen, W. J. Padilla, J. M. O. Zide, A. C. Gossard, A. J. Taylor, and R. D. Averitt, Nature (London) **444**, 597 (2006).
[12] H. T. Chen, W. J. Padilla, M. J. Cich, A. K. Azad, R. D. Averitt, and A. J. Taylor, Nature Photon. **3**, 148 (2009).
[13] J. G. Bednorz and K. A. Müller, Z. Phys. B: Condens. Matter **64**, 189 (1986).
[14] M. Ricci, N. Orloff, and S. M. Anlage, Appl. Phys. Lett. **87**, 034102 (2005).
[15] V. A. Fedotov, A. Tsiatmas, J. H. Shi, R. Buckingham, P. de Groot, Y. Chen, S. Wang, and N. I. Zheludev, Opt. Express **18**, 9015 (2010).
[16] D. R. Grischkowsky, S. R. Keiding, M. P. van Exter, and C. Fattinger, J. Opt. Soc. Am. B **7**, 2006 (1990).
[17] S. Linden, C. Enkrich, M. Wegener, J. Zhou, T. Koschny, and C. M. Soukolis, Science **306**, 1351 (2004).
[18] R. Singh, E. Smirnova, A. J. Taylor, J. F. O'Hara, and W. Zhang, Opt. Express **16**, 6537 (2008).
[19] R. Singh, A. K. Azad, J. F. O'Hara, A. J. Taylor, and W. Zhang, Opt. Lett. **33**, 1506 (2008).
[20] S.-Y. Chiam, R. Singh, J. Gu, J. Han, W. Zhang, and A. A. Bettiol1, Appl. Phys. Lett. **94**, 064102 (2009).
[21] R. Singh, Z. Tian, J. Han, C. Rockstuhl, J. Gu, and W. Zhang, Appl. Phys. Lett. **96**, 071114 (2010).
[22] A. K. Azad, J. Dai, and W. Zhang, Opt. Lett. **31**, 634 (2006).
[23] W. J. Padilla, A. J. Taylor, C. Highstrete, M. Lee, and R. D. Averitt, Phys. Rev. Lett. **96**, 107401 (2006).
[24] M. Walther, A. Ortner, H. Meier, U. Loffelmann, P. J. Smith, and J. G. Korvink, Appl. Phys. Lett. **95**, 251107 (2009).
[25] C. Rockstuhl, F. Lederer, C. Etrich, T. Zentgraf, J. Kuhl, and H. Giessen, Opt. Express **14**, 8827 (2006).
[26] J. Zhou, T. Koschny, and C. M. Soukoulis, Opt. Express **15**, 17881 (2007).
[27] F. London and H. London, Proc. R. Soc. London, Ser. A **152**, 24 (1935).
[28] M. A. Khazan, Ph.D. thesis, University of Hamburg, 2002.